Biological Psychiatry: Celebrating 50 Years

Archival Report

Mesolimbic Dopamine Function Is Related to Salience Network Connectivity: An Integrative Positron Emission Tomography and Magnetic Resonance Study

Robert A. McCutcheon, Matthew M. Nour, Tarik Dahoun, Sameer Jauhar, Fiona Pepper, Paul Expert, Mattia Veronese, Rick A. Adams, Federico Turkheimer, Mitul A. Mehta, and Oliver D. Howes

ABSTRACT

BACKGROUND: A wide range of neuropsychiatric disorders, from schizophrenia to drug addiction, involve abnormalities in both the mesolimbic dopamine system and the cortical salience network. Both systems play a key role in the detection of behaviorally relevant environmental stimuli. Although anatomical overlap exists, the functional relationship between these systems remains unknown. Preclinical research has suggested that the firing of mesolimbic dopamine neurons may activate nodes of the salience network, but in vivo human research is required given the species-specific nature of this network.

METHODS: We employed positron emission tomography to measure both dopamine release capacity (using the $D_{2/3}$ receptor ligand ^{11}C-PHNO, n = 23) and dopamine synthesis capacity (using ^{18}F-DOPA, n = 21) within the ventral striatum. Resting-state functional magnetic resonance imaging was also undertaken in the same individuals to investigate salience network functional connectivity. A graph theoretical approach was used to characterize the relationship between dopamine measures and network connectivity.

RESULTS: Dopamine synthesis capacity was associated with greater salience network connectivity, and this relationship was particularly apparent for brain regions that act as information-processing hubs. In contrast, dopamine release capacity was associated with weaker salience network connectivity. There was no relationship between dopamine measures and visual and sensorimotor networks, indicating specificity of the findings.

CONCLUSIONS: Our findings demonstrate a close relationship between the salience network and mesolimbic dopamine system, and they are relevant to neuropsychiatric illnesses in which aberrant functioning of both systems has been observed.

Keywords: ^{18}F-DOPA, Functional connectivity, Graph theory, ^{11}C-PHNO, Resting state, Striatum

https://doi.org/10.1016/j.biopsych.2018.09.010

Resting-state functional magnetic resonance imaging (rfMRI) has demonstrated that activity within networks of brain regions is temporally correlated even in the absence of explicit external demands (1) and furthermore that these networks underlie human cognition and behavior (2,3). The salience network, also referred to as the cingulo-opercular network, is centered around the anterior insula and dorsal anterior cingulate and in some instances has also been proposed to contain subcortical structures including the limbic (ventral) striatum and substantia nigra (4,5). Recent meta-analyses synthesizing structural and functional imaging data have identified this network as uniquely affected across psychiatric disorders (4,5).

The salience network plays a key role in identifying the most relevant internal and external stimuli to guide behavior appropriately (6–11). Connectivity within the salience network is increased by externally directed demands, which contrasts with the default mode network (centered around the ventromedial prefrontal cortex and the posterior cingulate cortex) (12,13), where connectivity is enhanced during self-generated thought (14,15). The salience network dynamically coordinates the activity of other networks, in particular switching away from the default mode to task-positive networks when appropriate, and impaired communication between the default mode and salience networks is seen in a range of disorders, including schizophrenia, drug addiction, and cognitive impairment (16–21).

Dopamine neurons also play a role in the identification of behaviorally relevant environmental stimuli. Mesolimbic dopamine neurons (projecting from the ventral tegmental area to the

SEE COMMENTARY ON PAGE 366

ISSN: 0006-3223

limbic striatum) have been proposed to signal reward prediction errors, which signal the discrepancy in the observed and predicted value of a stimulus (22). More recent research, however, has shown that these neurons respond to surprising stimuli even in the absence of any change in value, suggesting that their role extends to assigning salience to relevant environmental stimuli in general, not solely on the basis of value (23,24). Dysfunction of this system is also observed in many neuropsychiatric illnesses (25,26).

The need to develop an integrative understanding regarding the roles of the salience network and the mesolimbic dopamine system has been previously stressed (9). Given their overlap in function, it may be hypothesized that mesolimbic dopamine signaling plays a role in the modulation of the salience network. Recently, chemogenetic, optogenetic, and electrical stimulation of mesolimbic dopamine neurons in rodent models have been shown to activate salience network nodes, including regions not directly innervated by the ventral tegmental area (27–30). While cross-species similarities exist in the organization of cortical networks, there are also marked differences. Longer distance connections in particular are proportionally much weaker in primates, potentially contributing to an increased vulnerability to "disconnection syndromes" such as schizophrenia (31). As a result, in vivo human research is required for a comprehensive understanding of the relationship between network connectivity and neurochemical signaling. Human studies have demonstrated effects of pharmacological dopaminergic challenges on salience network connectivity, suggesting that dopamine might regulate the salience network in humans, but, crucially, these studies are limited in their explanatory potential because of the nonphysiological and anatomically nonspecific effects of the intervention (32–34). Thus, it remains unclear whether mesolimbic dopaminergic signaling is linked to the salience network in humans.

To address this, we employed positron emission tomography (PET) to measure both dopamine synthesis capacity and dopamine release capacity, and rfMRI to evaluate salience and default mode networks at rest in the same participants. Based on recent preclinical findings that stimulation of dopamine neurons projecting to the limbic striatum activates regions of the salience network (27–29), our primary hypothesis was that individuals with greater striatal dopamine synthesis and release capacity would show greater connectivity within the salience network, and, because of the reciprocal relationship between salience and default mode networks, weaker connectivity within the default mode network (27).

In addition, we identified within these networks regions that played the most important role in information processing ("hub nodes"). Hubs support the rapid integration of information across a complex system and as such can be considered an optimal target via which a network input may efficiently maximize its influence in a coordinated fashion (35,36). We therefore hypothesized that there would not be a uniform association between dopamine function and connectivity but that hub nodes would show the strongest association with dopamine function.

Given the preclinical emphasis on the mesolimbic dopamine projection, we focused on dopamine measures within the limbic striatum. However, we also explored the relationship between network connectivity and dopamine function in the associative and sensorimotor (dorsal) striatum. In addition, to provide a control condition, we investigated the relationship between striatal dopamine function and the visual and sensorimotor networks (networks not directly involved in salience processing), where we did not expect a relationship to be present.

METHODS AND MATERIALS

The experimental approach is summarized in Figures 1 and 2. PET was used to investigate two different aspects of dopaminergic functioning. In experiment 1, we measured dopamine synthesis capacity, while in experiment 2, we measured dopamine release capacity. rfMRI was used to investigate salience and default mode network connectivity. The relationship between salience and/or default mode connectivity and dopamine function was then investigated using a graph theoretical approach in which brain regions are represented as nodes and functional connections between these regions are represented as edges linking these nodes.

We first investigated whether network connectivity was associated with measures of dopamine function and identified specific nodes that were associated with dopamine function. We then separately classified nodes as information-processing hubs solely based on their pattern of rfMRI connectivity, and we determined whether dopamine-associated nodes overlapped significantly with these hub nodes.

In addition, the visual and sensorimotor networks were examined as control networks, as they are not directly involved in salience processing and show a lack of activation in preclinical studies of mesolimbic dopamine effects (27–29). Further details are given below and in the Supplement.

Experiment 1: Dopamine Synthesis Capacity

Participants underwent a PET scan with the ligand 3,4-dihydroxy-6-[^{18}F]fluoro-L-phenylalanine (^{18}F-DOPA). ^{18}F-DOPA PET measures the rate constant K_i^{cer} for ^{18}F-DOPA uptake, transport into synaptic vesicles, and its conversion into ^{18}F-dopamine, thus providing a measure of dopamine synthesis capacity (37).

A region-of-interest analysis was performed to determine the limbic striatum influx constant (K_i^{cer} [1/min]) (38). We also determined influx constants for associative and sensorimotor striatum, with these regions defined using the approach outlined by Martinez *et al.* (38).

Participants also underwent an rfMRI scan on a 3T GE Signa magnetic resonance scanner (GE Healthcare, Chicago, IL).

Experiment 2: Dopamine Release Capacity

Participants underwent two PET scans with the $D_{2/3}$ receptor ligand [^{11}C]-(+)-4-propyl-9-hydroxy-naphthoxazine (^{11}C-(+)-PHNO). A placebo scan gives a measure of baseline $D_{2/3}$ receptor availability (nondisplaceable binding potential [BP_{ND}]), while a scan following dexamphetamine administration allows quantification of the change in BP_{ND} due to competition from increased synaptic dopamine concentrations. The percentage reduction in $D_{2/3}$ receptor availability between placebo and dexamphetamine scans thus provides an

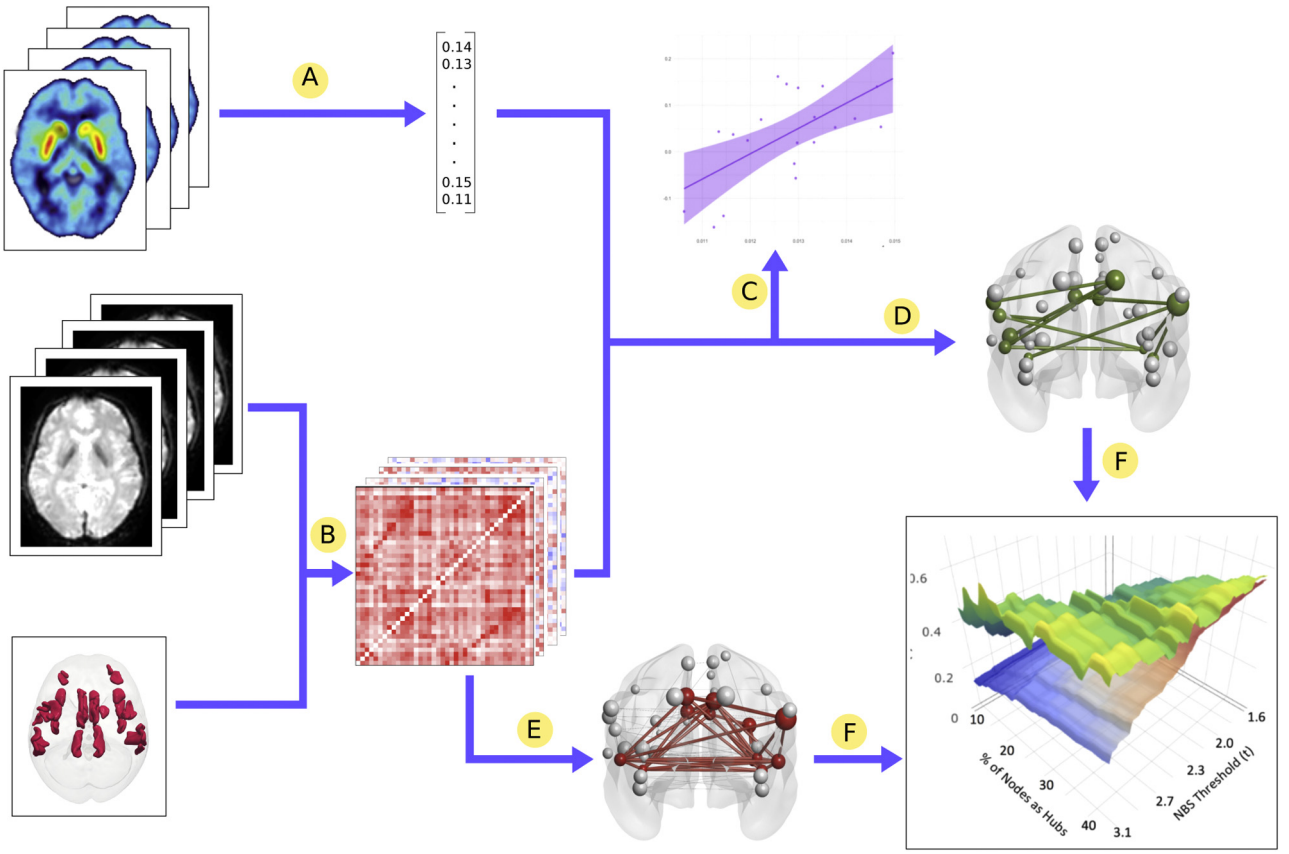

Figure 1. Summary of methods. **(A)** K_i^{cer} or change in nondisplaceable binding potential (ΔBP_{ND}) obtained for each participant from positron emission tomography data. **(B)** Resting-state functional magnetic resonance imaging time courses extracted from salience network nodes and individual functional connectivity graphs constructed for each participant. **(C)** Relationship between salience network average strength and dopamine measure investigated. **(D)** Dopamine-associated subnetworks identified using network-based statistics (NBS). **(E)** Hub nodes identified from resting-state functional magnetic resonance imaging data. **(F)** Overlap between hub nodes and dopamine-associated subnetworks investigated.

index of dopamine release capacity. We calculate the percent change in BP_{ND} as follows:

$$\Delta BP_{ND} = 100 \times \frac{BP_{ND\,(baseline)} - BP_{ND\,(dexamphetamine)}}{BP_{ND\,(baseline)}}\%$$

Either placebo or 0.5 mg/kg dexamphetamine was administered orally 3 hours before ^{11}C-(+)-PHNO administration, so that scan acquisition coincided with the expected time of peak action (39). ΔBP_{ND} was measured in the same regions as in experiment 1.

Participants also underwent an rfMRI scan using a Siemens MAGNETOM Verio 3T scanner (Siemens Corp., Erlangen, Germany).

Common Methods

Participants. Participants had no previous or current history of psychiatric illness (assessed by the Structured Clinical Interview for DSM-IV Axis I Disorders).

Magnetic Resonance Imaging Analysis. Time series were extracted from 333 predefined nodes of interests of the Gordon cortical atlas. The salience and default mode network nodes of the Gordon atlas are displayed in Supplemental Figure S1. For each participant, a graph representing a functional connectivity network was constructed, each edge representing the level of functional connectivity between a pair of nodes. To demonstrate the robustness of our findings, we also replicated all analyses using two alternative atlases—the Power (40) and CONN network (41) atlases. Furthermore, in addition to using the a priori defined network labels for each node (e.g., salience, default mode), we also ran a whole-brain community detection algorithm for each atlas (42) to generate definitions of the salience and default mode networks based on the connectivity patterns present in the current data sets, and we repeated our analyses using these data-driven node assignments.

Network Strength and Dopamine Function. For each participant and each network, average network strength was defined as the mean z-transformed Pearson's correlation coefficient between all network nodes (i.e., mean edge strength) (43). We first calculated Pearson correlation coefficients between network average strength and the PET measures of dopamine function. We then tested whether the correlation between network strength and dopamine function was

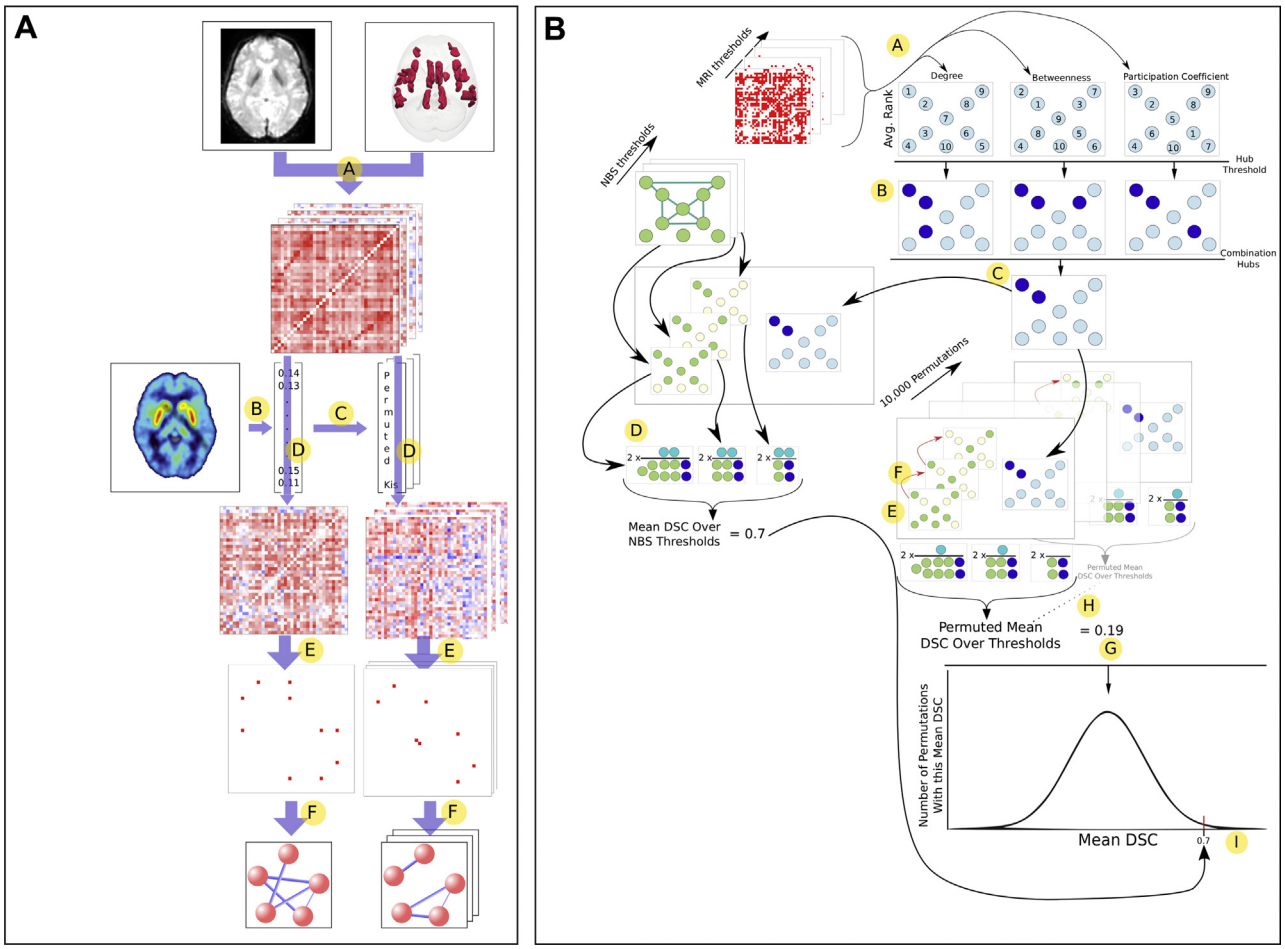

Figure 2. Methods for **(A)** identifying dopamine-associated nodes using the network-based statistic (NBS) and **(B)** identifying overlap between dopamine-associated nodes and hub nodes. Methods are described for ^{18}F-DOPA and salience network but are identical for ^{11}C-PHNO and other networks. A, Individual functional connectivity graphs constructed for the salience network from resting-state functional magnetic resonance imaging (rfMRI) data for each participant. B, Limbic K_i^{cer} obtained for each participant from positron emission tomography (PET) data. C, K_i^{cer} randomly permuted 10,000 times. D, Group PET-MRI graph constructed; each edge represents the correlation between that edge's functional connectivity and the limbic K_i^{cer} values (Ki). E, PET-MRI graphs thresholded and binarized. F, Number of edges of the largest connected component in both the actual PET-MRI graph (five edges in the illustrated example) and the permuted graphs (three edges in the example) compared. The p values were calculated based on the proportion of permuted examples the true example is larger than. A, Each node is ranked according to degree, betweenness centrality, and participation coefficient at each MRI threshold. The average rank across thresholds for each metric is then calculated. B, Nodes thresholded at a given rank; here the top-ranked 30% are chosen. C, Determine which nodes pass the threshold for all three metrics, here 20% of nodes classified as "combination hubs." D, Calculate the Dice similarity coefficient (DSC) between the "combination hubs" and the nodes that form part of the dopamine subnetwork previously identified (Figure 1A). Do this for each NBS threshold and calculate the average DSC across thresholds. E, Randomly pick a selection of nodes equal in number to the number of nodes in the subnetwork at the most lenient NBS threshold. F, Match the number of nodes in this random selection to that in the subnetwork at more stringent thresholds by randomly deleting a node (red arrow) when necessary to match.

significantly different between default mode and salience networks using the method described by Meng *et al.* as implemented in the cocor (1.1-3) package for R 3.3.2 (44,45). We also investigated the correlation between dopamine measures and salience–default mode "balance" (salience network average strength minus default mode network average strength).

Identifying Dopamine-Associated Nodes. To identify whether specific nodes show a significant relationship with limbic dopamine synthesis capacity, we used the network-based statistic to investigate salience, default mode, sensorimotor, and visual networks separately (see Figure 2A and Supplemental Methods) (46). Within each network, we identified subnetworks showing a significant relationship with dopamine function; we term these "dopamine-associated subnetworks," and the nodes within these networks "dopamine-associated nodes." In addition to examining intranetwork connectivity, we used the same approach to examine salience and default mode internetwork connectivity. To ensure the robustness of the results, this approach was undertaken across a range of network-based statistic thresholds (100 thresholds, t = 1.3–3.1, equivalent to p = .2–.005 for n = 23), where weaker thresholds will capture subnetworks showing a

widespread diffuse relationship with dopamine function, and more stringent thresholds identify smaller clusters showing the strongest relationship.

Identifying Network Hubs. Based on the patterns of resting-state connectivity within the salience and default mode networks, we then calculated several graph metrics to identify network hubs. We calculated node degree (47), betweenness centrality (47), and participation coefficient (48). We termed a node that ranked highly on all three metrics a "combination hub" (Figure 2B steps A–C), highlighting its importance as an all-round information-processing node. By varying the stringency of criteria used to defined nodes as hubs, we defined sets of combination hubs comprising between 10% and 40% of the total number of nodes.

Identifying Overlap Between Dopamine-Associated Nodes and Network Hubs. We next asked whether dopamine-associated nodes were statistically more likely to be combination hubs. We quantified the overlap of dopamine-associated nodes and combination hubs using the Dice similarity coefficient (where A is the set of dopamine-associated nodes and B is the set of combination-hub nodes) (49,50):

$$\textit{Dice Similarity Coefficient} = \frac{2|A \cap B|}{|A| + |B|}$$

The Dice coefficient was calculated for each of the 100 network-based statistic thresholds (t = 1.3–3.1) and then averaged to give a single score (Figure 2B part D). Permutation testing was used to test whether this overlap score was statistically significant. This procedure was then repeated for each of the combination-hub thresholds (10%–40%), thereby giving a p value for each hub threshold.

We also investigated whether there was a significant overlap between ^{18}F-DOPA and ^{11}C-(+)-PHNO dopamine-associated nodes.

RESULTS

Participants

Twenty-one participants took part in experiment 1, the ^{18}F-DOPA study (mean [SD] age = 23.5 years [3.36 years]; 67% male). Twenty-three participants took part in experiment 2, the ^{11}C-(+)-PHNO study (mean [SD] age = 24.4 years [4.5 years]; 57% male).

Network Strength and Dopamine Function

Experiment 1: Dopamine Synthesis Capacity (^{18}F-DOPA). The correlations between edge strength and limbic dopamine synthesis capacity are displayed in the lower triangle of Figure 3A. Average network strength of the salience network positively correlated with limbic dopamine synthesis capacity (r_p = .51, p = .017, Figure 3B), and this was also significant for all other parcellations (r_p = .44–.62) (Supplemental Figure S3). In contrast, average network strength of the default mode network did not show a significant relationship with limbic dopamine synthesis capacity (r_p = −.32, p = .16) (Figure 3B).

The correlation between dopamine synthesis capacity and salience network average strength was significantly different from that between dopamine synthesis capacity and default mode average network strength (z = −2.7, p = .008). Furthermore, salience–default mode balance (salience network average strength minus default mode network average strength) correlated with dopamine synthesis capacity (r_p = .60, p = .004) (Figure 3B).

When the relationship between salience network average strength and dopamine synthesis capacity in other striatal regions was investigated, the findings were significant for the associative striatum (r_p = .46, p = .034) but not the sensorimotor striatum (r_p = .43, p = .053) (Supplemental Figure S2). As hypothesized, there was no association between limbic dopamine synthesis capacity and average network strength of either the visual (r_p = .05, p = .85) or sensorimotor (r_p = .09, p = .68) networks.

Experiment 2: Dopamine Release Capacity [^{11}C-(+)-PHNO]. The correlations between edge strength and limbic dopamine release capacity are displayed in the upper triangle of Figure 3A. Contrary to our hypothesis, average network strength of the salience network was negatively correlated with limbic dopamine release capacity (r_p = −.42, p = .049) (Figure 3B), a finding that was also significant for some (Gordon data–driven, Power data–driven) but not all (Power a priori, CONN) of the alternative parcellations (r_p = −.24 to −.52) (Supplemental Figure S3). There was no significant correlation between dopamine release capacity and default mode average network strength (r_p = .03, p = .9). The difference between these two correlations was not significant (z = 1.43, p = .15), and salience–default mode balance did not correlate significantly with dopamine release capacity (r_p = −.29, p = .18).

As in experiment 1, salience network strength was significantly associated with dopamine release capacity in the associative striatum (r_p = −.5, p = .015) but showed no relationship with the sensorimotor striatum (r_p = −.17, p = .44) (Supplemental Figure S2). Furthermore, as in experiment 1, there were no associations between limbic dopamine release capacity and average network strength in either the visual (r = −.27, p = .22) or sensorimotor (r = −.28, p = .20) networks. Interestingly, however, in an exploratory analysis, dopamine release capacity within the sensorimotor striatum showed a significant relationship with sensorimotor network average strength (r = −.58, p = .004).

There was no relationship between rfMRI motion and either network strength or dopamine measures (results in the Supplement).

Identifying Dopamine-Associated Nodes

Experiment 1: Dopamine Synthesis Capacity (^{18}F-DOPA). Using the network-based statistic, we identified salience network subnetworks showing a significant positive relationship with limbic dopamine synthesis capacity across a range of thresholds (Figure 3D). In contrast, subnetworks within the default mode network showed a significant negative relationship with dopamine synthesis capacity.

We also used the network-based statistic to examine internetwork connections between default mode and salience networks. At specific thresholds, greater dopamine synthesis capacity was associated with weaker internetwork connectivity

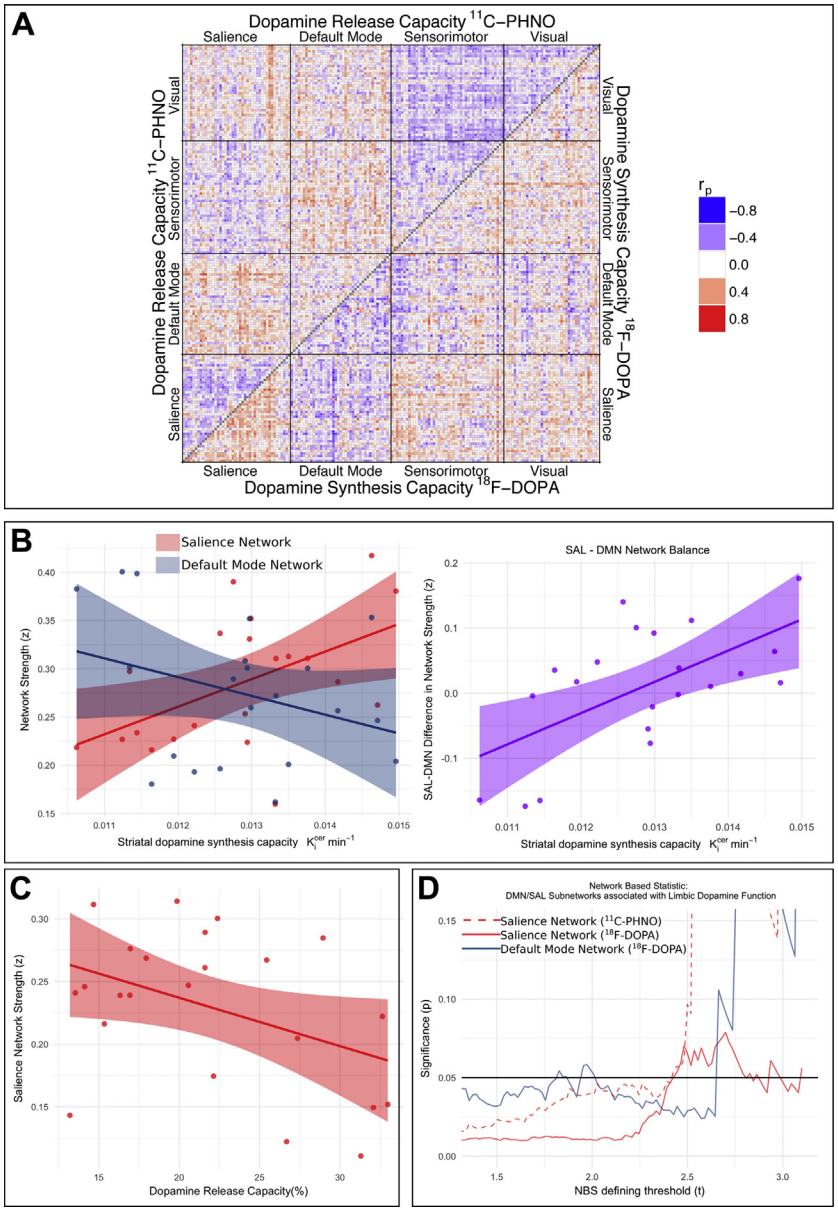

Figure 3. Resting-state networks and their relationship with limbic dopamine function. **(A)** Dopamine-associated graphs—each edge represents the correlation between that edge's resting-state functional magnetic resonance imaging functional connectivity values and limbic dopamine synthesis and/or release capacity. **(B)** Dopamine synthesis capacity is correlated with salience network (SAL) strength ($n = 21$, $r_p = .51$, $p = .017$), did not correlate with default mode network (DMN) strength ($r_p = -.32$, $p = .16$), and is positively correlated with the difference between SAL strength and DMN strength ($r_p = .60$, $p = .004$). **(C)** Dopamine release capacity negatively correlated with SAL strength ($r_p = -.42$, $p = .049$). **(D)** Network-based statistic (NBS) identifies subnetworks significantly associated with dopamine synthesis and/or release capacity across a range of thresholds.

(i.e., greater decoupling), although this was not significant across a wide range of thresholds (Supplemental Figure S4).

When dopamine synthesis capacity in other striatal subdivisions was examined, the findings were again significant for the associative but not sensorimotor striatum (Supplemental Figure S5). The specificity of the findings was again demonstrated by the fact that no dopamine-associated subnetworks were identified in either visual ($p > .29$ for all thresholds) or sensorimotor ($p > .38$) networks.

Experiment 2: Dopamine Release Capacity [^{11}C-(+)-PHNO]. We identified subnetworks within the salience network showing a significant negative relationship with limbic dopamine release capacity (Figure 3D). No default mode subnetworks showed a significant association with dopamine release capacity. As in experiment 1, examination of internetwork connections suggested that release capacity was associated with internetwork coupling only at specific thresholds, and in this case greater release capacity was associated with stronger coupling (Supplemental Figure S4).

Dopamine release in other regions was examined, and similarly to experiment 1, significant results were observed for the salience network with the dopamine measure in the associative striatum but not sensorimotor striatum (Supplemental Figure S5). As before, we demonstrated the specificity of findings in that no visual ($p > .12$ all thresholds) or sensorimotor subnetwork ($p > .11$ all thresholds) was associated with limbic dopamine release capacity.

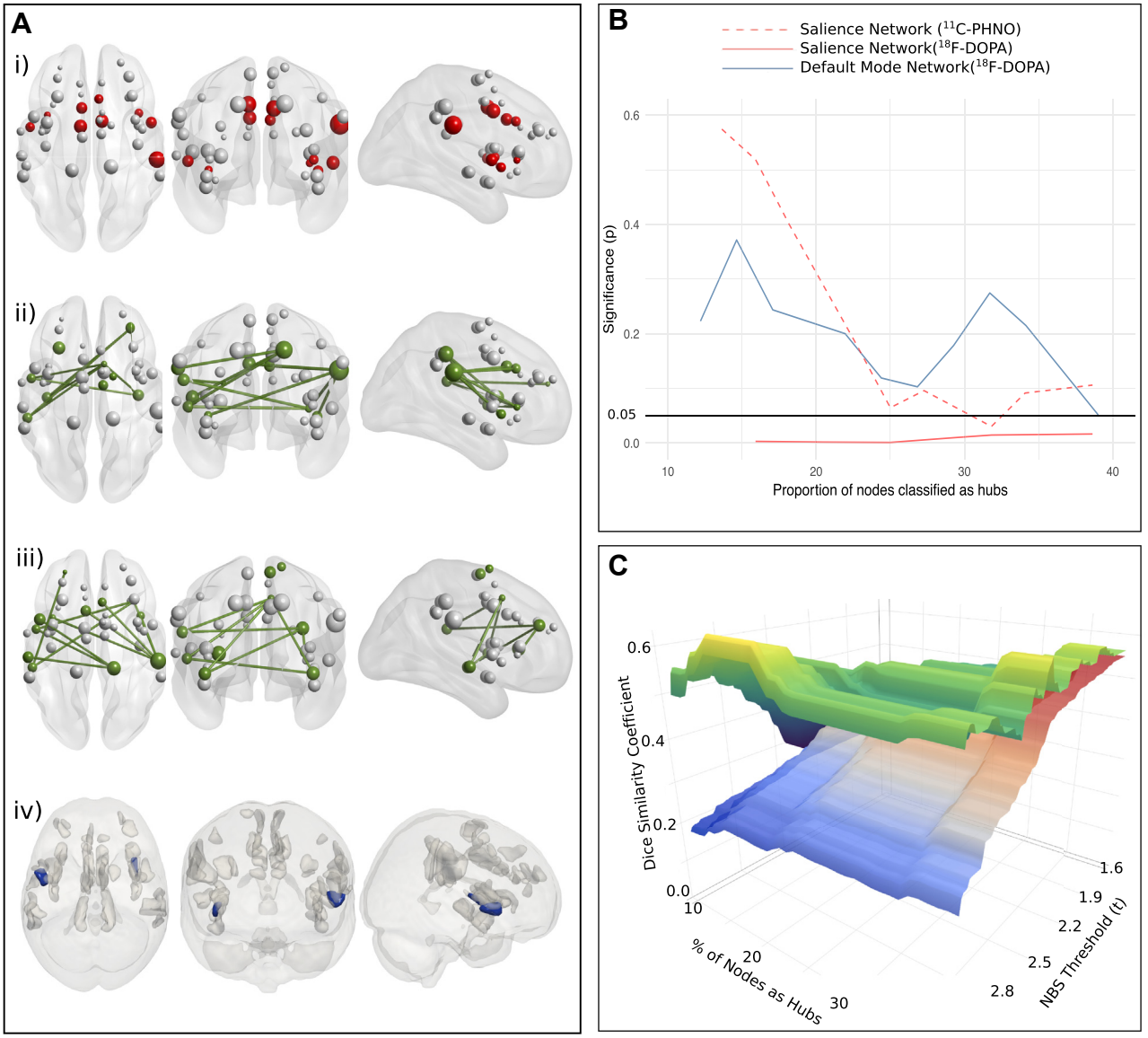

Figure 4. Characterization of dopamine-associated subnetworks. **(A)** Salience-network hubs and dopamine-associated subnetworks: red nodes represent network combination hubs and green nodes and edges represent the dopamine-associated network, in which edge strength correlates with limbic dopamine synthesis capacity. i) Hub nodes in experiment 1; ii) dopamine-associated network in experiment 1 at a specific network-based statistic (NBS) threshold; iii) dopamine-associated network in experiment 2; iv) Two nodes classified as both dopamine-associated nodes and hub nodes in both experiments at the most stringent threshold. **(B)** Graph displaying whether overlap between dopamine-associated nodes and combination hubs is significant. **(C)** Illustrating the overlap between salience network hub nodes and nodes involved in for ^{18}F-DOPA-associated subnetworks. The top (green-yellow) layer represents the Dice similarity coefficients for the observed dopamine-associated nodes and the combination-hub nodes, while the bottom (blue-red) layer represents the mean overlap coefficients of 10,000 randomized networks. In this figure, the Dice coefficient is plotted individually for each NBS threshold (i.e., not averaged as in the construction of Figure 3B).

In both experiments, these findings were seen in various parcellations and methods of node assignment (Supplemental Figure S6).

Identifying Overlap Between Dopamine-Associated Nodes and Network Hubs

Experiment 1: Dopamine Synthesis Capacity (^{18}F-DOPA). We next investigated whether the dopamine-associated nodes identified in the previous step overlapped significantly with nodes that were classified as information-processing hubs. Within the salience network, we found that regardless of how many nodes were defined as hubs within our range of investigation (i.e., the top-ranked 10%–40%), these nodes were likely to be dopamine-associated nodes, and this overlap was significantly more likely than expected by chance for all hub thresholds (Figure 4B), and this was the case for all parcellations and methods of node assignment (Supplemental Figure S7). The Dice coefficient between nodes in salience–^{18}F-DOPA subnetworks and

combination hubs across a range of thresholds is shown in Figure 4C, illustrating that the nodes that are most strongly associated with dopamine synthesis capacity (i.e., those surviving the more stringent network-based statistic thresholds) are also the most likely to be key information-processing hubs (as defined by resting-state functional connectivity).

The Dice coefficient between combination hubs and the dopamine-associated nodes within the default mode network was numerically greater than the Dice coefficient of the random network at all thresholds, but this difference was statistically significant only for certain hub thresholds and parcellations (see Figure 4B and Supplemental Figure S7).

Experiment 2: Dopamine Release Capacity [^{11}C-(+)-PHNO]. The Dice coefficient between combination hubs and the salience–^{11}C-(+)-PHNO subnetworks were numerically greater than the mean overlap expected of the random network, but this difference was statistically significant only for certain thresholds and parcellations (Figure 4B and Supplemental Figure S7).

Overlap Between Experiments. Dice overlap scores between the ^{11}C-(+)-PHNO– and ^{18}F-DOPA–associated nodes ranged from 0.36 at the most stringent network-based statistic threshold where equal node networks existed (number of nodes = 11) to 0.92 at the least stringent threshold (number of nodes = 36). None of these overlaps was greater than would be expected by chance ($p > .20$ for all thresholds). We then investigated which nodes were in dopamine-associated networks at the most stringent threshold and were also combination hubs (ranked in the top 11/40 nodes in both experiments). Only two nodes fulfilled these criteria; these were located bilaterally in the insula (see Figure 4A part iv).

DISCUSSION

Using rfMRI and a dual-tracer PET paradigm, we demonstrate a strong relationship between limbic dopamine function and salience network functional connectivity in humans. Both the salience network and mesolimbic dopamine system are central to the pathophysiology of various neuropsychiatric disorders (4,5,25,26). To our knowledge, however, this is the first human study to both measure limbic dopamine function and investigate its relationship with the salience network.

Specifically, we demonstrated that stronger connectivity within the salience network was directly associated with limbic dopamine synthesis capacity and, contrary to our initial hypothesis, was inversely associated with limbic dopamine release capacity. Furthermore, the biological relevance of this result is supported by the finding that there was significant overlap between nodes in salience subnetworks associated with dopamine synthesis capacity and nodes separately identified as information-processing hubs. We also identified default mode subnetworks in which edge strength was inversely correlated with synthesis capacity.

The Relationship Between Mesolimbic Dopamine Function and the Salience Network

The current study advances our understanding regarding the relationship between mesolimbic dopamine activity and salience network function. Preclinical studies have suggested a link between mesolimbic dopamine function and nodes of the salience network (27–29). However, a precise homologue of the salience network is not present in rodent models, because of both the species-specific nature of cortical networks and the fact that in humans the network is characterized by the presence of Von Economo neurons, a distinct set of pyramidal neurons, which are not observed in rodents (31,51,52). Previous studies in humans have used rfMRI in combination with pharmacological manipulations of the dopamine system (32,53–55). Without the use of PET, however, it is not possible to obtain a measure of the dopaminergic effect of the pharmacological intervention, which can vary significantly between individuals for the same dose. Furthermore, drug challenges perturb the system widely, causing various neurochemical changes across the brain and affecting neurovascular coupling (56). In contrast, our resting-state data were obtained in a drug-free state, and ^{18}F-DOPA PET indexes physiological dopamine function.

Although previous studies have integrated PET and the examination of resting-state networks, these have predominantly obtained only measures of baseline dopamine receptor availability (57–60). Two studies have measured dopamine function but did not examine the relationship with the salience network (34,61).

Dopamine-Synthesis and Release Capacity

We hypothesized that release and synthesis capacity would capture similar facets of a single construct—the activity of an individual's mesolimbic dopamine system. Our finding of divergent relationships between these two measures and salience network connectivity does not support this interpretation. Both release and synthesis capacity are complex signals, and the relationship between the two is not clear (62,63). Synthesis capacity represents the rate of 3,4-dihydroxy-L-phenylalanine decarboxylation, and it depends on the number of dopaminergic neurons and their mean firing rate. Measures of release capacity will be determined by the reactivity of mesolimbic dopamine neurons to the effects of amphetamine. Agonist tracers such as ^{11}C-(+)-PHNO preferentially bind to the high-affinity state of the D_2 receptor (64,65). This means that our measure of percentage release could be affected by the proportion of D_2 receptors in a high-affinity state as well as the level of dopamine release. Future studies combining antagonist and agonist radiotracers would help determine the potential influence of interindividual differences in the proportion of D_2 receptors in the high-affinity state. A tentative hypothesis that unites our findings assumes that in a healthy individual, dopamine synthesis capacity reflects a summary measure of tonic dopamine neuron firing and appropriate adaptive phasic firing, while release capacity reflects that individual's propensity for spontaneous phasic firing in the absence of behaviorally relevant stimuli (66). Taken with the finding that reduced salience network connectivity is observed in disorders of aberrant salience processing, this suggests a model in which greater salience network connectivity is associated with the appropriate attribution of salience, mediated by robust adaptive dopaminergic signaling, while a propensity for stimulus-independent dopamine neuron firing is

associated with weakening of the network and misattribution of salience (67–71). This is a speculative interpretation, however, and assumes that the consequences of higher dopamine synthesis capacity in healthy participants differ from those in patient populations where it has been linked to disorders of salience (72).

Dopamine Pathways

Preclinical research has often focused on the dopamine neurons of the ventral tegmental area. The limbic striatum is a major projection target for these neurons and, as such, an appropriate region of focus. In rodents, however, the mesolimbic pathway is proportionally larger than in humans, and therefore, although the associative striatum receives dopaminergic innervation from the nigra, parts of the human midbrain-associative striatum pathway are homologous to the rodent mesolimbic pathway (73,74). As a result, it is not surprising that the relationship observed between the salience network and limbic dopamine function was also seen when using measures of associative striatum dopamine function. No relationship, however, was seen with dopamine measures obtained from the sensorimotor striatum and salience network connectivity, although an association was seen with release capacity in this region and sensorimotor network connectivity, suggesting a degree of functional specificity in the relationship between dopamine measures and network connectivity.

Clinical Implications

Structural and functional abnormalities within the salience network are a common biological substrate of mental illness and exist transdiagnostically across a broad range of disorders, including depression, schizophrenia, and Parkinson's disease (4,5,75–77). The mesolimbic dopamine system is also affected in these disorders (25,26,78,79). Our finding that the two systems show coupling in humans could explain why they are disordered in several illnesses, as dysfunction in any one of the network's nodes could conceivably lead to impairment across both systems. Our findings also highlight opportunities for the development of pharmacological interventions. The ability to link the effects of quantifiable neurochemical modulation to change in network function raises the possibility of mapping receptor actions to desired network alterations.

Limitations and Further Questions

Given that the firing of mesolimbic neurons has been shown to provoke widespread neural activity in regions receiving no direct dopaminergic innervation (29), our findings could be interpreted as indicating that mesolimbic dopaminergic signaling is able to regulate salience network function. However, while differences in dopaminergic tone could feasibly shift the balance between the two networks, it is not possible for us to infer the direction of causality.

Likewise, the precise site of relevant dopaminergic activity is not clear. ^{11}C-(+)-PHNO and ^{18}F-DOPA are unable reliably characterize dopamine function outside of the striatum, and it was therefore not possible to test whether a relationship between direct dopaminergic innervation of network nodes and network connectivity also existed.

We used an eyes-closed resting-state scan, and some networks have shown greater reliability when participants have kept eyes open. The differences are relatively small, however, and therefore unlikely to have significantly influenced our findings (80).

The use of acute dopaminergic challenges during simultaneous PET and MRI would allow for the study of intraindividual effects of dopaminergic release on network average strength and organization and may help to disentangle some of these issues. Studies in clinical populations, such as individuals with schizophrenia, where measures of both dopaminergic and network function may show wider ranges (81), and the inclusion of behavioral tests would help further determine the relevance of these findings to pathophysiology and psychopathology.

Measures of dopamine function showed strong associations with salience network connectivity, and in the case of dopamine synthesis capacity, this was particularly the case for nodes that were identified as information-processing hubs within the salience network. These findings are relevant to developing integrated models of brain function in health and disease and for the development of treatments that attempt to restore network function via neurochemical modulation.

ACKNOWLEDGMENTS AND DISCLOSURES

This work is supported by the Wellcome Trust (Grant No. 200102/Z/15/Z [to RAM]) and the National Institute for Health Research (NIHR) (to MMN) and a EU-FP7 MC-ITN IN-SENS grant (Grant No. 607616 [to TD]) and by the NIHR at Oxford Health National Health Service Foundation Trust. RAA is funded by an NIHR University College London Hospitals Biomedical Research Centre Postgraduate Fellowship. This study was funded by Medical Research Council-UK (Grant No. MC-A656-5QD30 [to ODH]), Wellcome Trust (Grant No. 094849/Z/10/Z [to ODH]), NIHR Biomedical Research Centre at South London, Maudsley NHS Foundation Trust, and King's College London. The views expressed are those of the authors and not necessarily those of the NHS, the NIHR, or the Department of Health.

ODH has received investigator-initiated research funding from or participated in advisory and/or speaker meetings organized by AstraZeneca, Autifony Therapeutics, Bristol-Myers Squibb, Eli Lilly, Heptares, Janssen Pharmaceuticals, Lundbeck, Leyden Delta, Otsuka, Servier, Sunovion Pharmaceuticals, RAND Corporation, and Roche. Neither ODH nor any member of his family has been employed by or has holdings and/or a financial stake in any biomedical company. MAM has consulted for Cambridge Cognition, Lundbeck, and FORUM Pharmaceuticals in the past 3 years. He has also received research funding from Takeda, Eli Lilly, and Roche. The other authors report no biomedical financial interests or potential conflicts of interest.

ARTICLE INFORMATION

From the Department of Psychosis Studies (RAM, MMN, SJ, FP, ODH) and Department of Neuroimaging (FP, MV, FT, MAM), Institute of Psychiatry, Psychology and Neuroscience, Kings College London, De Crespigny Park; Psychiatric Imaging Group (RAM, MMN, TD, SJ, ODH), MRC London Institute of Medical Sciences, Hammersmith Hospital; Faculty of Medicine (RAM, MMN, TD, SJ, ODH), Institute of Clinical Sciences; Department of Mathematics (PE); and EPSRC Centre for Mathematics of Precision Healthcare (PE), Imperial College London; Institute of Cognitive Neuroscience (RAA) and Division of Psychiatry (RAA), University College London, London; and Department of Psychiatry (TD), University of Oxford, Warneford Hospital, Oxford, United Kingdom.

Address correspondence to Robert A. McCutcheon, M.R.C.Psych., Box 67, Department of Psychosis Studies, Institute of Psychiatry, Psychology and Neuroscience, Kings College London, De Crespigny Park, London SE5 8AF, UK; E-mail: robert.mccutcheon@kcl.ac.uk.

RAM and MMN contributed equally to this work.

Received Jul 31, 2018; revised Sep 10, 2018; accepted Sep 14, 2018.

Supplementary material cited in this article is available online at https://doi.org/10.1016/j.biopsych.2018.09.010.

REFERENCES

1. Cordes D, Haughton VM, Arfanakis K, Wendt GJ, Turski PA, Moritz CH, *et al.* (2000): Mapping functionally related regions of brain with functional connectivity MR imaging. AJNR Am J Neuroradiol 21:1636–1644.
2. Park H-J, Friston K (2013): Structural and functional brain networks: From connections to cognition. Science 342:1238411.
3. Bassett DS, Sporns O (2017): Network neuroscience. Nat Neurosci 20:353–364.
4. McTeague LM, Huemer J, Carreon DM, Jiang Y, Eickhoff SB, Etkin A (2017): Identification of common neural circuit disruptions in cognitive control across psychiatric disorders. Am J Psychiatry 174:676–685.
5. Goodkind M, Eickhoff SB, Oathes DJ, Jiang Y, Chang A, Jones-Hagata LB, *et al.* (2015): Identification of a common neurobiological substrate for mental illness. JAMA Psychiatry 72:305–315.
6. Kennerley SW, Walton ME, Behrens TEJ, Buckley MJ, Rushworth MFS (2006): Optimal decision making and the anterior cingulate cortex. Nat Neurosci 9:940–947.
7. Augustine JR (1996): Circuitry and functional aspects of the insular lobe in primates including humans. Brain Res Brain Res Rev 22: 229–244.
8. Bossaerts P (2010): Risk and risk prediction error signals in anterior insula. Brain Struct Funct 214:645–653.
9. Palaniyappan L (2012): Does the salience network play a cardinal role in psychosis? An emerging hypothesis of insular dysfunction. J Psychiatry Neurosci 37:17–27.
10. Hyman JM, Holroyd CB, Seamans JK (2017): A novel neural prediction error found in anterior cingulate cortex ensembles. Neuron 95:447–456, e3.
11. Uddin LQ (2015): Salience processing and insular cortical function and dysfunction. Nat Rev Neurosci 16:55–61.
12. Menon V, Uddin LQ (2010): Saliency, switching, attention and control: A network model of insula function. Brain Struct Funct 214:655–667.
13. Sridharan D, Levitin DJ, Menon V (2008): A critical role for the right fronto-insular cortex in switching between central-executive and default-mode networks. Proc Natl Acad Sci U S A 105:12569–12574.
14. Greicius MD, Krasnow B, Reiss AL, Menon V (2003): Functional connectivity in the resting brain: A network analysis of the default mode hypothesis. Proc Natl Acad Sci U S A 100:253–258.
15. Andrews-Hanna JR, Smallwood J, Spreng RN (2014): The default network and self-generated thought: Component processes, dynamic control, and clinical relevance. Ann N Y Acad Sci 1316:29–52.
16. Sripada RK, Swain JE, Evans GW, Welsh RC, Liberzon I (2014): Childhood poverty and stress reactivity are associated with aberrant functional connectivity in default mode network. Neuropsychopharmacology 39:2244–2251.
17. Jilka SR, Scott G, Ham T, Pickering A, Bonnelle V, Braga RM, *et al.* (2014): Damage to the salience network and interactions with the default mode network. J Neurosci 34:10798–10807.
18. Chand GB, Wu J, Hajjar I, Qiu D (2017): Interactions of the salience network and its subsystems with the default-mode and the central-executive networks in normal aging and mild cognitive impairment. Brain Connect 7:401–412.
19. Liang X, He Y, Salmeron BJ, Gu H, Stein EA, Yang Y (2015): Interactions between the salience and default-mode networks are disrupted in cocaine addiction. J Neurosci 35:8081–8090.
20. Bonnelle V, Ham TE, Leech R, Kinnunen KM, Mehta MA, Greenwood RJ, Sharp DJ (2012): Salience network integrity predicts default mode network function after traumatic brain injury. Proc Natl Acad Sci U S A 109:4690–4695.
21. O'Neill A, Mechelli A, Bhattacharyya S (2018): Dysconnectivity of large-scale functional networks in early psychosis: A meta-analysis [published online ahead of print Jul 3]. Schizophr Bull.
22. Schultz W, Dayan P, Montague PR (1997): A neural substrate of prediction and reward. Science 275:1593–1599.
23. Howes OD, Nour MM (2016): Dopamine and the aberrant salience hypothesis of schizophrenia. World Psychiatry 15:3–4.
24. Takahashi YK, Batchelor HM, Liu B, Khanna A, Morales M, Schoenbaum G (2017): Dopamine neurons respond to errors in the prediction of sensory features of expected rewards. Neuron 95:1395–1405, e3.
25. Volkow ND, Wise RA, Baler R (2017): The dopamine motive system: Implications for drug and food addiction. Nat Rev Neurosci 18: 741–752.
26. Salamone JD, Correa M (2012): The mysterious motivational functions of mesolimbic dopamine. Neuron 76:470–485.
27. Roelofs TJM, Verharen JPH, van Tilborg GAF, Boekhoudt L, van der Toorn A, de Jong JW, *et al.* (2017): A novel approach to map induced activation of neuronal networks using chemogenetics and functional neuroimaging in rats: A proof-of-concept study on the meso-corticolimbic system. Neuroimage 156:109–118.
28. Helbing C, Brocka M, Scherf T, Lippert MT, Angenstein F (2016): The role of the mesolimbic dopamine system in the formation of blood-oxygen-level dependent responses in the medial prefrontal/anterior cingulate cortex during high-frequency stimulation of the rat perforant pathway. J Cereb Blood Flow Metab 36:2177–2193.
29. Lohani S, Poplawsky AJ, Kim S-G, Moghaddam B (2017): Unexpected global impact of VTA dopamine neuron activation as measured by opto-fMRI. Mol Psychiatry 22:585–594.
30. Decot HK, Namboodiri VM, Gao W, McHenry JA, Jennings JH, Lee S-H, *et al.* (2017): Coordination of brain wide activity dynamics by dopaminergic neurons. Neuropsychopharmacology 42: 615–627.
31. Horvát S, Gămănuț R, Ercsey-Ravasz M, Magrou L, Gămănuț B, Van Essen DC, *et al.* (2016): Spatial embedding and wiring cost constrain the functional layout of the cortical network of rodents and primates. PLoS Biol 14:e1002512.
32. Cole DM, Beckmann CF, Oei NYL, Both S, van Gerven JMA, Rombouts SARB (2013): Differential and distributed effects of dopamine neuromodulations on resting-state network connectivity. Neuroimage 78:59–67.
33. Cole DM, Oei NYL, Soeter RP, Both S, Van Gerven JMA, Rombouts SARB, Beckmann CF (2013): Dopamine-dependent architecture of cortico-subcortical network connectivity. Cereb Cortex 23:1509–1516.
34. Schrantee A, Ferguson B, Stoffers D, Booij J, Rombouts S, Reneman L (2016): Effects of dexamphetamine-induced dopamine release on resting-state network connectivity in recreational amphetamine users and healthy controls. Brain Imaging Behav 10:548–558.
35. Gao J, Liu Y-Y, D'Souza RM, Barabási A-L (2014): Target control of complex networks. Nat Commun 5:5415.
36. van den Heuvel MP, Sporns O (2013): Network hubs in the human brain. Trends Cogn Sci 17:683–696.
37. Kumakura Y, Cumming P (2009): PET studies of cerebral levodopa metabolism: A review of clinical findings and modeling approaches. Neuroscientist 15:635–650.
38. Martinez D, Slifstein M, Broft A, Mawlawi O, Hwang D, Huang Y, *et al.* (2003): Imaging human mesolimbic dopamine transmission with positron emission tomography. Part II: Amphetamine-induced dopamine release in the functional subdivisions of the striatum. J Cereb Blood Flow Metab 23:285–300.
39. Asghar SJ, Tanay VAMI, Baker GB, Greenshaw A, Silverstone PH (2003): Relationship of plasma amphetamine levels to physiological, subjective, cognitive and biochemical measures in healthy volunteers. Hum Psychopharmacol 18:291–299.
40. Power JD, Cohen AL, Nelson SSM, Wig GS, Barnes KA, Church JA, *et al.* (2011): Functional network organization of the human brain. Neuron 72:665–678.
41. Whitfield-Gabrieli S, Nieto-Castanon A (2012): Conn: A functional connectivity toolbox for correlated and anticorrelated brain networks. Brain Connect 2:125–141.
42. Blondel VD, Guillaume JL, Lambiotte R, Lefebvre E (2008): Fast unfolding of communities in large networks. J Stat Mech 2008: P10008.

43. Lord LD, Allen P, Expert P, Howes O, Lambiotte R, McGuire P, *et al.* (2011): Characterization of the anterior cingulate's role in the at-risk mental state using graph theory. Neuroimage 56:1531–1539.
44. Meng X, Rosenthal R, Rubin DB (1992): Comparing correlated correlation coefficients. Psychol Bull 111:172–175.
45. Diedenhofen B, Musch J (2015): Cocor: A comprehensive solution for the statistical comparison of correlations. PLoS One 10:e0121945.
46. Zalesky A, Fornito A, Bullmore ET (2010): NeuroImage network-based statistic : Identifying differences in brain networks. Neuroimage 53:1197–1207.
47. Freeman LC (1978): Centrality in social networks conceptual clarification. Soc Netw 1:215–239.
48. Guimera R, Nunes Amaral L (2005): Functional cartography of complex metabolic networks. Nature 433:895–900.
49. Dice LR (1945): Measures of the amount of ecologic association between species. Ecology 26:297–302.
50. Jann K, Gee DG, Kilroy E, Schwab S, Smith RX, Cannon TD, Wang DJJ (2015): Functional connectivity in BOLD and CBF data: SIMILARITY and reliability of resting brain networks. Neuroimage 106:111–122.
51. Nimchinsky EA, Gilissen E, Allman JM, Perl DP, Erwin JM, Hof PR (1999): A neuronal morphologic type unique to humans and great apes. Proc Natl Acad Sci U S A 96:5268–5273.
52. Dijkstra AA, Lin LC, Nana AL, Gaus SE, Seeley WW (2018): Von Economo neurons and fork cells: A neurochemical signature linked to monoaminergic function. Cereb Cortex 28:131–144.
53. Williams D (2002): Dopamine-dependent changes in the functional connectivity between basal ganglia and cerebral cortex in humans. Brain 125:1558–1569.
54. Achard S, Bullmore E (2007): Efficiency and cost of economical brain functional networks. PLoS Comput Biol 3:0174–0183.
55. Tost H, Braus DF, Hakimi S, Ruf M, Vollmert C, Hohn F, Meyer-Lindenberg A (2010): Acute D2receptor blockade induces rapid, reversible remodeling in human cortical-striatal circuits. Nat Neurosci 13:920–922.
56. Nordin LE, Li TQ, Brogren J, Johansson P, Sjögren N, Hannesdottir K, *et al.* (2013): Cortical responses to amphetamine exposure studied by pCASL MRI and pharmacokinetic/pharmacodynamic dose modeling. Neuroimage 68:75–82.
57. Nagano-Saito A, Lissemore JI, Gravel P, Leyton M, Carbonell F, Benkelfat C (2017): Posterior dopamine D2/3 receptors and brain network functional connectivity. Synapse 71:1–13.
58. Kaiser RH, Treadway MT, Wooten DW, Kumar P, Goer F, Murray L, *et al.* (2018): Frontostriatal and dopamine markers of individual differences in reinforcement learning: A multi-modal investigation. Cereb Cortex 28:4281–4290.
59. Kohno M, Okita K, Morales AM, Robertson CL, Dean AC, Ghahremani DG, *et al.* (2016): Midbrain functional connectivity and ventral striatal dopamine D2-type receptors: Link to impulsivity in methamphetamine users. Mol Psychiatry 21:1554–1560.
60. Cole DM, Beckmann CF, Searle GE, Plisson C, Tziortzi AC, Nichols TE, *et al.* (2012): Orbitofrontal connectivity with resting-state networks is associated with midbrain dopamine D3 receptor availability. Cereb Cortex 22:2784–2793.
61. Dang LC, O'Neil JP, Jagust WJ (2012): Dopamine supports coupling of attention-related networks. J Neurosci 32:9582–9587.
62. Berry AS, Shah VD, Furman DJ, White RL III, Baker SL, O'Neil JP, *et al.* (2018): Dopamine synthesis capacity is associated with D2/3 receptor binding but not dopamine release. Neuropsychopharmacology 43:1201–1211.
63. Piccini P, Pavese N, Brooks DJ (2003): Endogenous dopamine release after pharmacological challenges in Parkinson's disease. Ann Neurol 53:647–653.
64. Seeman P (2012): Dopamine agonist radioligand binds to both D2High and D2Low receptors, explaining why alterations in D2High are not detected in human brain scans. Synapse 66:88–93.
65. Slifstein M, Abi-Dargham A (2018): Is it Pre- or Postsynaptic? Imaging Striatal Dopamine Excess in Schizophrenia. Biol Psychiatry 83: 635–637.
66. Maia TV, Frank MJ (2017): An Integrative Perspective on the Role of Dopamine in Schizophrenia. Biol Psychiatry 81:52–66.
67. Moran LV, Tagamets MA, Sampath H, O'Donnell A, Stein EA, Kochunov P, Hong LE (2013): Disruption of anterior insula modulation of large-scale brain networks in schizophrenia. Biol Psychiatry 74: 467–474.
68. Orliac F, Naveau M, Joliot M, Delcroix N, Razafimandimby A, Brazo P, *et al.* (2013): Links among resting-state default mode network, salience network, and symptomatology in schizophrenia. Schizophr Res 148:74–80.
69. White TP, Joseph V, Francis ST, Liddle PF (2010): Aberrant salience network (bilateral insula and anterior cingulate cortex) connectivity during information processing in schizophrenia. Schizophr Res 123:105–115.
70. Manoliu A, Riedl V, Zherdin A, Mühlau M, Schwerthöffer D, Scherr M, *et al.* (2014): Aberrant dependence of default mode/central executive network interactions on anterior insular salience network activity in schizophrenia. Schizophr Bull 40:428–437.
71. Wang C, Ji F, Hong Z, Poh JS, Krishnan R, Lee J, *et al.* (2016): Disrupted salience network functional connectivity and white-matter microstructure in persons at risk for psychosis: Findings from the LYRIKS study. Psychol Med 46:2771–2783.
72. McCutcheon R, Beck K, Jauhar S, Howes OD (2018): Defining the locus of dopaminergic dysfunction in schizophrenia: A meta-analysis and test of the mesolimbic hypothesis. Schizophr Bull 44:1301–1311.
73. Nauta WJH, Smith GP, Faull RLM, Domesick VB (1978): Efferent connections and nigral afferents of the nucleus accumbens septi in the rat. Neuroscience 3:385–401.
74. Ikeda H, Saigusa T, Kamei J, Koshikawa N, Cools AR (2013): Spiraling dopaminergic circuitry from the ventral striatum to dorsal striatum is an effective feed-forward loop. Neuroscience 241:126–134.
75. Chang YT, Lu CH, Wu MK, Hsu SW, Huang CW, Chang WN, *et al.* (2018): Salience network and depressive severities in Parkinson's disease with mild cognitive impairment: A structural covariance network analysis. Front Aging Neurosci 9:1–11.
76. Palaniyappan L, Simmonite M, White TP, Liddle EB, Liddle PF (2013): Neural primacy of the salience processing system in schizophrenia. Neuron 79:814–828.
77. Brugger SP, Howes OD (2017): Heterogeneity and homogeneity of regional brain structure in schizophrenia. JAMA Psychiatry 74:1104–1111.
78. Nestler EJ, Carlezon WA (2006): The mesolimbic dopamine reward circuit in depression. Biol Psychiatry 59:1151–1159.
79. Jauhar S, Nour MM, Veronese M, Rogdaki M, Bonoldi I, Azis M, *et al.* (2017): A test of the transdiagnostic dopamine hypothesis of psychosis using positron emission tomographic imaging in bipolar affective disorder and schizophrenia. JAMA Psychiatry 74:1206–1213.
80. Patriat R, Molloy EK, Meier TB, Kirk GR, Nair VA, Meyerand ME, *et al.* (2013): The effect of resting condition on resting-state fMRI reliability and consistency: A comparison between resting with eyes open, closed, and fixated. Neuroimage 78:463–473.
81. Jauhar S, Veronese M, Nour MM, Rogdaki M, Hathway P, Turkheimer FE, *et al.* (2018): Determinants of treatment response in first-episode psychosis: An ^{18}F-DOPA PET study [published online ahead of print Apr 20]. Mol Psychiatry.